

Article

Effects of Precipitation and Topography on Total Phosphorus Loss from Purple Soil

Xiaowen Ding ^{1,2,*}, Ying Xue ¹, Ming Lin ¹ and Yuan Liu ¹

¹ Key Laboratory of Regional Energy and Environmental Systems Optimization, Ministry of Education, North China Electric Power University, Beijing 102206, China; astridxuey@163.com (Y.X.); linming000000@163.com (M.L.); ly921105@gmail.com (Y.L.)

² Institute for Energy, Environment and Sustainable Communities, University of Regina, Regina, SK S4S 7H9, Canada

* Correspondence: binger2000dxw@hotmail.com; Tel.: +86-10-6177-2982

Academic Editors: Gordon Huang and Yurui Fan

Received: 7 April 2017; Accepted: 27 April 2017; Published: 28 April 2017

Abstract: The Sichuan Basin is the main agricultural production area of the upper reaches of the Yangtze River and is also an extremely important ecological area because it is rich in biodiversity and has complex and diverse landscape types. The dominant soil type, purple soil, is prone to rapid soil erosion and weathering processes because it is shallow and rich in phosphorus and other nutrients. Field experiments were conducted to reveal the effects of precipitation and topography characteristics on nonpoint source pollutants from purple soil. The results showed that total phosphorus (TP) load and TP concentration both increased with increasing rainfall amount, and there was an initial time of runoff and sediment yield before runoff generation. Moreover, the TP load generally increased with precipitation intensity as setting a coincident value of rainfall amount; however, the difference between TP load at 30 and 60 mm/h was minimal as was the difference between 90 and 120 mm/h. Similarly, TP concentration increased with increasing precipitation intensity. In terms of topographical conditions, TP load increased with increasing gradient, but began to decline when the gradient was about 20°, which indicates that 20° is the critical gradient for TP loss. There was a significant positive correlation between gradient and TP concentration when the gradient was <15°, whereas the increase in TP concentration slowed as the gradient increased.

Keywords: total phosphorus; precipitation; topography; purple soil; precipitation simulation; Sichuan Basin

1. Introduction

With the development of modern agriculture technology, the use of chemical fertilizers and pesticides in agriculture is increasing and the chemical composition becomes more complicated, which lead to wide range of nonpoint source (NPS) pollution after long-term accumulation in the soil [1–3]. Due to the large area of cultivated land and multi-sources, widespread and difficulty in processing of NPS pollution, it has been the main type of water pollution when point source pollution control is becoming more and more effective [4–6]. In recent years, more and more studies focus on the migration of NPS pollutants, which could put forward theoretical guidance for NPS control and water pollution treatment [7–9]. Existing researches show that the main factors affecting NPS pollutants migration are precipitation and topography, and precipitation is the main motivation of NPS pollutants migration, the topography affects the migration of NPS pollutants by gravity flow [10,11].

The Yangtze River is the longest river in China with abundant natural resources, such as hydro-power resources, biological resources and mineral resources, and agricultural production in Yangtze River basin plays an important role in China [12,13]. Meanwhile, Sichuan Basin is an important

agricultural and ecological region of the upper reaches of Yangtze River [14]. The type of agricultural production in Sichuan Basin is intensive, which mainly depends on nutrients such as nitrogen and phosphorus fertilizers [15]. In addition, the Sichuan Basin has very complex landscape types because of its special geographical location, and it has rich biodiversity and widely distributed mountains and plains [16]. Purple soil is the main soil type in Sichuan Basin, which account for 68% of total cultivated land [17]. This kind of soil is vulnerable to the effects of weathering and erosion because of its superficial distribution and distributing in region of high rainfall amount [18]. Furthermore, purple soil contains phosphorus, potassium and other minerals, among which phosphorus is an important part of the NPS pollutants in the process of soil erosion, including the application of phosphate fertilizer in farmland [19]. Total phosphorus (TP) occurs in dissolved state in rainfall runoff, and occurs in adsorbed state when it adsorbs on the sediments [20–22]. The main source of TP in Sichuan Basin is the utilization of fertilizers and pesticides, as well as some organic phosphorus output from forests and grasslands. Meanwhile, the main loss of TP is caused by soil erosion and other driving forces. Therefore, it is of great significance for the prevention of agricultural NPS pollutants and the protection of water resources to study on TP loss in purple soil erosion under different precipitation and topography conditions [23].

In the past few decades, many researchers have focused on the precipitation, topography conditions on the influence of the NPS pollutants migration [24–26]. A prediction of potential bioavailable P in the water columns and sediments and their relations with enzymatic hydrolysis was conducted and the spatial variations of phosphorus showed that higher phosphorus content and more intense enzymatic hydrolysis in silty clay finer sediments [27]. A significant increase has been observed in dissolved phosphorus concentration of storm flow with storm intensity (0.09–0.16 mg/L), which suggests that phosphorus release from soil and/or runoff of the watershed increases with storm size [28]. Qian et al. found that phosphorus loss was determined by the concentration and the runoff volume; moreover, the main form of phosphorus loss was particulate phosphorus [29]. A study carried out on a hillslope cropland region in the Sichuan Basin indicated that total bioavailable phosphorus loss and the rate of phosphorus by overland flow decreased with increasing vegetation coverage [30]. A small-plot rainfall simulation study was conducted at three sites in Alberta, Canada, and determined that soil test phosphorus, TP, and dissolved reactive phosphorus concentration in runoff increased with manure concentration for fresh and residual manure [31]. However, previous studies mostly used drainage basin as the unit of study area to study the influence of precipitation, topography and land use conditions on NPS pollutants migration. But less researches focused on a specific soil type, such as purple soil region. Therefore, in this paper, field experiment was used to carry out research into the influence of different precipitation and topography on TP loss in purple soil region.

This study focused on the effects of different precipitation and topography conditions on TP loss in the purple soil region. Field experiment was used to simulate the influence of precipitation and topography conditions in reality. Precipitation conditions were divided into different rainfall amount and different precipitation intensity. Topography conditions were expressed by gradient (tilt angle of slope surface and horizontal plane). By means of simulating precipitation and topography conditions, this study focused on the variation tendency of TP load and concentration to explain the effects of rainfall amount, precipitation intensity and gradient on TP loss. This research has great significance in the establishment of the NPS pollutants models, the rate of model parameters and the analysis of pollution results. Furthermore, it is helpful to understand NPS pollutants migration and could provide the technical support for decision makers on the control and treatment of NPS pollutants under different natural conditions.

2. Materials and Methods

2.1. Experimental Devices

Generally, the area of small-scale artificial precipitation experiments is less than 10 m². As for the runoff simulation experiments, the average range for the length of the soil box is 1–2 m, the range of

the width is 0.5–1 m and the range of the depth is 0.22–0.5 m [32]. Hence, the size of the soil box in this study was designed as $1.0 \times 0.6 \times 0.25 \text{ m}^3$ (Figure 1). The soil boxes were installed wheels and screw rods, the former were to facilitate the transportation of boxes and the screw rods were connected with soil boxes by nuts, which could adjust the slant angle of soil boxes. In order to simulate rainfall runoff better, soil boxes were punched on the side to make the sediment migrate freely. There are 4 rows of holes, each row with 8 holes and the diameter of each hole was 5 mm. In the meantime, the bottom of soil boxes extended outward 0.1 m to collect runoff from holes on the side of boxes. Then, small buckets were used to collect sediments and runoff to conduct the subsequent measurement.

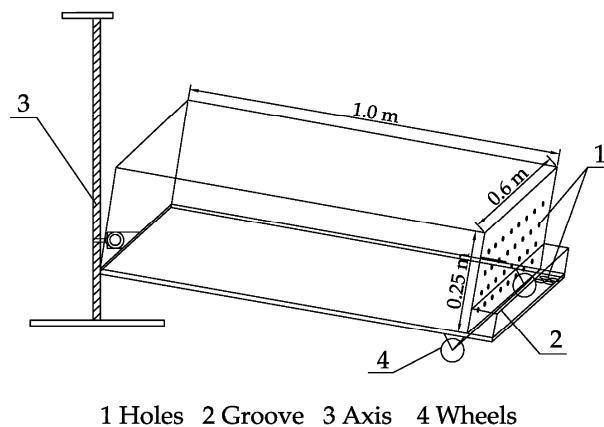


Figure 1. Schematic showing the design of the soil boxes.

Norton nozzle-type rainfall simulator was used in this study. This rainfall simulator was divided into water supply systems and spray systems, and it consisted of sprinkler, small power machine, pressure gauge, water supply pipe, water hose and so on (Figure 2) [33]. Sprinkler was set at a height of 2.5 m and a hydraulic pressure of 0.04 MPa to make sure the precipitation was similar to the size and distribution of the raindrops in nature when the nozzle swung. The precipitation intensity could be set to different levels by changing the frequency of nozzle swings and kept stable to remain in the set condition.

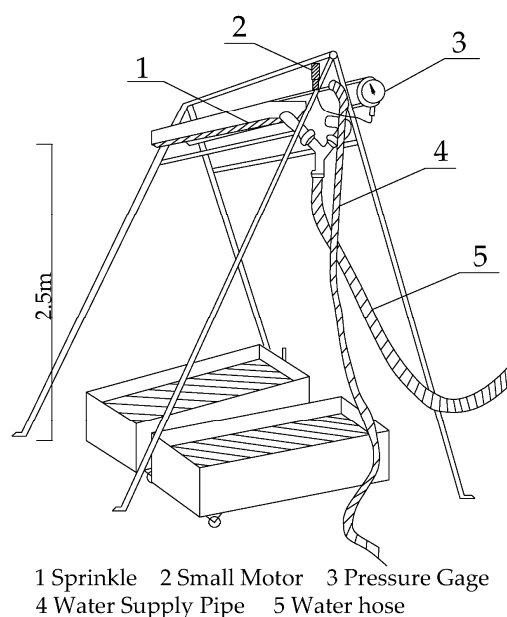


Figure 2. Schematic of the Norton nozzle-type rainfall simulator.

2.2. Experimental Materials

Purple soil is a type of soil that has high fertility, however, it is vulnerable to water erosion and weathering in the Sichuan Basin due to the large rainfall amount [18]. In this study, the experimental site was located on a slope in Beibei, Chongqing (106°43'E, 29°83'N) (Figure 3), an eastern part of the Sichuan Basin, where it is easy to form soil erosion and severe NPS pollution due to steep slopes and abundant precipitation [34]. The temperature of Chongqing was about 8.2 °C in the experimental period. In Chongqing, the percentages of different land uses were showed in the Table 1.

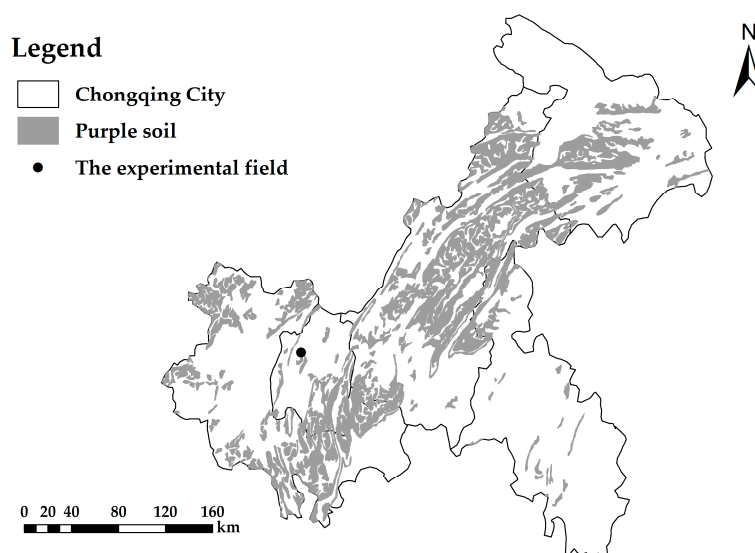


Figure 3. Distribution of purple soil in the Chongqing City and the location of experimental site.

Table 1. Percentages of different land uses in Chongqing (%).

Percentage (Total)	Agricultural Land				Construction Land	Unused Land
	Cultivated Field	Woodland	Grassland	Else		
100	29.66	45.98	4.03	9.01	10.88	0.44

Surface soil within 20 cm was used in this study due to the superficial distribution of purple soil. On the one hand, it could maintain the typical nature of purple soil, on the other hand, it could be helpful to reduce the spatial heterogeneity between different soil layers. Soil samples need to be pretreated. The physical and chemical properties of soil samples are shown in Table 2. First, it was necessary to grind the obtained soil with a grinder and then remove the stones and impurities from the soil with a 7-mm mesh screen. Second, the initial moisture content of the soil was reduced to 12.16% by oven drying method, which was similar to the actual soil moisture. Finally, the soil was stirred evenly to form soil samples. After pretreating, the soil was loaded into the soil boxes, 5 cm soil layer each time, and used ring cutting method to measure the soil bulk density. To make sure it was similar to nature, the soil bulk density should be remained at 1.30 g/L. Then, 5 cm soil layer was load into the boxes after the soil was loosed with the steel fork. This load was carried out for 5 times, and the soil bulk density was measured after each loading to keep it uniform and constant. At the same time, the soil should be loose after each loading to prevent soil agglomeration which could lead to soil stratification.

Table 2. Physical and chemical properties of soil samples.

Soil Layer (cm)	Unit Weight (g/cm ³)	Initial Soil Moisture Rate (%)	Organic Matter (g/kg)	TP (g/kg)	pH
0–20	1.30	12.16	8.75	0.68	5.5

2.3. Experimental Methods

According to the precipitation data of Chongqing (National Meteorological Information Center) in recent years, the maximum precipitation intensity in some areas of Chongqing could reach more than 100 mm/h. In addition, the precipitation intensity range of Norton nozzle-type rainfall simulator was 30~150 mm/h, so 4 kinds of precipitation intensity were chosen in this study: 30, 60, 90, 120 mm/h. As for the design of gradient, the topography of study area varied in a large range, and it is forbidden to cultivate crops on steep gradients above 25 degrees according to Law of The People's Republic of China on Water and Soil Conservation. Therefore, 5 kinds of gradient were chosen in this precipitation experiment: 5°, 10°, 15°, 20° and 25°. Then the simulated precipitation conditions and topography conditions were combined for a total of 20 rains. The combination of precipitation and gradient in each scenario is shown in Table 3. In this study, the runoff time was controlled at 40 min, and different precipitation duration was determined according to the initial runoff time. During the experiment, the runoff was collected every 5 min until the end of the experiment and was measured at the end of the precipitation. In order to reduce the impact of the soil moisture, bulk density and other physical and chemical properties of the experiment to ensure the accuracy of the experiment, new soil was reloaded after each precipitation experiment and the experimental soil returned to nature.

Table 3. Scheme of artificial precipitation experiments.

Precipitation Intensity (β)	30 mm/h (β_1)	60 mm/h (β_2)	90 mm/h (β_3)	120 mm/h (β_4)
Gradient (α)				
5° (α_1)	$\alpha_1\beta_1$	$\alpha_1\beta_2$	$\alpha_1\beta_3$	$\alpha_1\beta_4$
10° (α_2)	$\alpha_2\beta_1$	$\alpha_2\beta_2$	$\alpha_2\beta_3$	$\alpha_2\beta_4$
15° (α_3)	$\alpha_3\beta_1$	$\alpha_3\beta_2$	$\alpha_3\beta_3$	$\alpha_3\beta_4$
20° (α_4)	$\alpha_4\beta_1$	$\alpha_4\beta_2$	$\alpha_4\beta_3$	$\alpha_4\beta_4$
25° (α_5)	$\alpha_5\beta_1$	$\alpha_5\beta_2$	$\alpha_5\beta_3$	$\alpha_5\beta_4$

The phosphorus determined in the experiment included dissolved phosphorus that dissolved in the rainfall runoff and adsorbed phosphorus that adsorbed on the sediments. After obtaining the water sample, the water sample was filtered and divided into supernatant containing dissolved phosphorus and deposit carrying adsorbed phosphorus. Then, the concentration of dissolved phosphorus and adsorbed phosphorus were measured, and the concentrations were multiplied by the volume of supernatant and sediment respectively to get the TP load. After that, TP load was divided by the total volume of water samples to get the TP concentration which took mg/L as unit.

2.4. Data

According to Section 2.3, it is necessary to separate the concentration of dissolved phosphorus in the supernatant and the concentration of adsorbed phosphorus in the sediments to obtain the load and concentration data of TP in each scenario. Water quality-determination of total phosphorus- ammonium molybdate spectrophotometric method was used to measure the dissolved phosphorus in the supernatant, and soil-determination of total phosphorus by alkali fusion Mo-Sb Anti spectrophotometric method for the adsorption of phosphorus in the sediment. After the TP load and TP concentration in each scenario were obtained, the data were processed by SPSS software to reveal the effects of precipitation and topography on TP load and TP concentration.

As far as dissolved phosphorus in the water samples was concerned, its concentration was measured by ammonium molybdate spectrophotometric method. The processes for determining concentration of dissolved phosphorus were as follows. Firstly, a calibration curve was drew by absorbance of different concentrations of phosphate standard solution comparing with a zero concentration solution. Secondly, samples were took and added potassium persulfate and nitric acid-perchloric acid respectively for digestion. And then, ascorbic acid solution and molybdate solution were added into digestion solution. After that, the solutions were placed in room temperature for

15 min, and the path for 30 mm cuvette was used for determining absorbance after deducting the absorbance of zero concentration solution at the wavelength of 700 nm. Afterwards, the concentrations of water samples were achieved by the equation (national standard *water quality-determination of total phosphorus- ammonium molybdate spectrophotometric method* GB 11893-89):

$$C = \frac{m}{V} \quad (1)$$

where C was TP content (mg/L), m was the phosphorus content of sample (μg), V was sample volume for determination (mL).

As for adsorbed phosphorus, its concentration was measured by alkali fusion Mo-Sb Anti spectrophotometric method. Firstly, the sample was melted after adding sodium hydroxide for specimen preparation. Secondly, a calibration curve was drew by absorbance of different concentrations of phosphate standard solution comparing with a zero concentration solution. Thirdly, samples and blank test were taking to measure absorbance contrast with calibration curve. After that, the concentrations of sediment samples were achieved by the equation (national standard *soil-determination of total phosphorus by alkali fusion Mo-Sb Anti spectrophotometric method* HJ 632-2011):

$$\omega = \frac{[(A - A_0) - a] \times V_1}{b \times m \times w_{dm} \times V_2} \quad (2)$$

where ω was the TP content of sample (mg/kg), A was absorbance of specimen, A_0 was absorbance of blank test, a was the intercept of the calibration curve, V_1 was constant volume of specimen (mL), b was the gradient of the calibration curve, m was the sample amount (g), V_2 was sample volume (mL), w_{dm} was sediment mass fraction (%).

3. Results

3.1. The Effects of Rainfall Amount on TP

3.1.1. The Effects of Rainfall Amount on TP Load

In the process of soil and water loss, dissolved phosphorus, including dissolved organic phosphorus, orthophosphate and polyphosphate, was transported by dissolving into the rainfall runoff. And the adsorbed phosphorus was the major form of phosphorus loss which was transported by adsorbing on the sediments. The effects of rainfall amount on TP load on different gradients under different precipitation intensities are showed in the Figure 4. The rainfall amounts on a gradient under different precipitation intensities were integrated into one line to eliminate the influence of precipitation intensity on TP load.

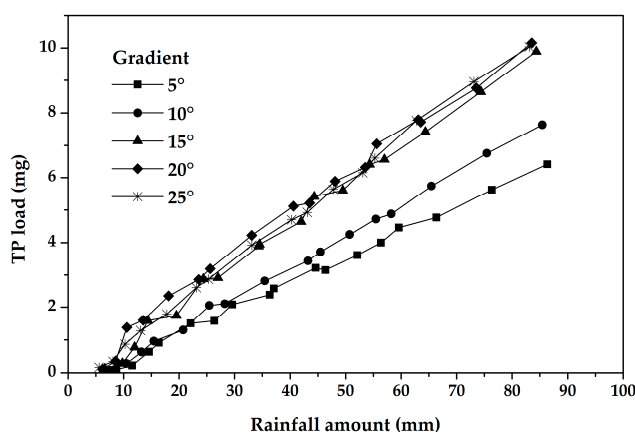


Figure 4. Correlations between rainfall amount and TP load on different gradients under different precipitation intensities.

Under the different gradient conditions, the correlation between rainfall amount and TP load was positive, which represented that TP increased with the increase of rainfall amount under various gradient levels (Table 4). This may be due to the more dissolved phosphorus dissolving with rainfall amount increasing and soil moisture increasing. Meanwhile, increased rainfall runoff made heavier scouring effect on soil, a lot of dissolved phosphorus flowed away with rainfall runoff and a large amount of adsorbed phosphorus lost with sediments. These all made TP load increased with the increase of rainfall amount, therefore, the more rainfall amount occurred, the more rainfall runoff and sediments yielded, and the heavier TP loss was. Moreover, there were slight differences of TP load between different gradients, which indicated that landform was an important factor of TP loss (See Section 3.3.1).

Table 4. Correlations between TP load and rainfall amount on different gradients.

Gradient	Correlation	Correlation Coefficient
5°	$y = 0.0805x - 0.4916$	0.9956
10°	$y = 0.0969x - 0.6441$	0.9985
15°	$y = 0.1253x - 0.5322$	0.9940
20°	$y = 0.1253x - 0.1895$	0.9926
25°	$y = 0.1282x - 0.4751$	0.9983

As can be seen in Figure 4, there all existed initial time of runoff and sediments yield before rainfall runoff was generated in each gradients, which is caused by the delayed rainfall runoff after onset of precipitation. At the beginning of the precipitation, the rainwater fell to the surface of the soil and began to infiltrate, meanwhile, the soil moisture was relatively low and the soil moisture was in an unsaturated state. Therefore, the precipitation continued to infiltration and the rainfall runoff was not generated immediately. With the increase of rainfall amount, soil moisture reached saturation, rainfall runoff generated and TP began to lose.

3.1.2. The Effects of Rainfall Amount on TP Concentration

The effects of rainfall amount on TP concentration under different gradients conditions are shown in Figure 5.

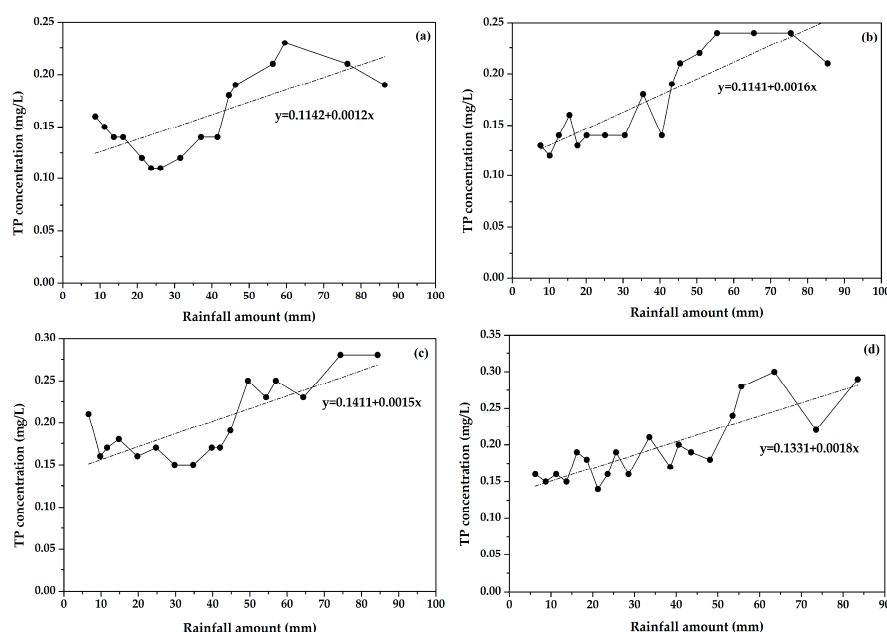


Figure 5. Cont.

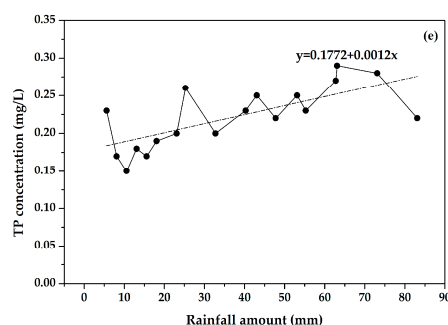


Figure 5. Correlations between rainfall amount and TP concentrations on gradients of (a) 5°; (b) 10°; (c) 15°; (d) 20°; and (e) 25° under different precipitation intensities.

According to the trend line in Figure 5, the TP concentration increased with increasing rainfall amount, which was similar to the effect of rainfall amount on TP load. And this increase was meant that the increase of TP loss was more than the increase of rainfall amount. With the increase of rainfall amount, the dynamic potential energy of sediments increased and the loss of sediment in rainfall runoff increased, and the amount of adsorbed phosphorus increased. Therefore, the increased rainfall amount would carry more TP since adsorbed phosphorus was the main form of TP. And the effects of landform on TP concentration were discussed in Section 3.3.2.

3.2. The Effects of Precipitation Intensity

3.2.1. The Effects of Precipitation Intensity on TP Load

Considering the direct correlation between precipitation intensity and rainfall amount, the effect of precipitation intensity on TP load was very similar to the effect of rainfall amount on TP load in a certain precipitation duration, and the effect of rainfall amount on TP load was doped to a certain extent. Therefore, this study controlled the rainfall amount and set the rainfall amount to a fixed value to study the effect of different precipitation intensities on TP loss under fixed rainfall amount condition. And under this condition, different precipitation intensities corresponding to different precipitation durations, which would lead to different levels of TP load in each gradient condition. The effects of precipitation intensities on TP load is shown in Figure 6 under different gradient conditions.

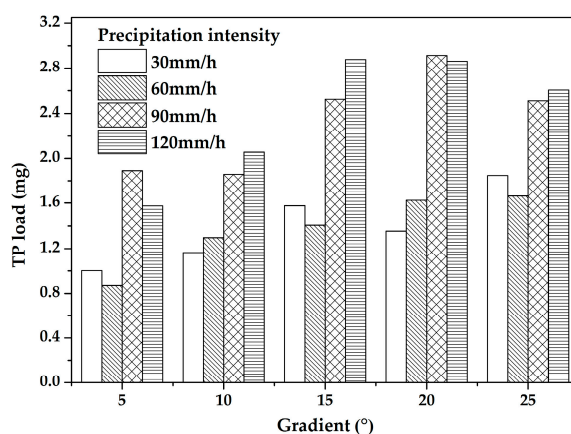


Figure 6. Correlation between precipitation intensity and TP load under various gradients.

We found that TP load generally increased with an increase in precipitation intensity. However, the difference between TP load at 30 and 60 mm/h was minimal as was that between 90 and 120 mm/h. The reason for the small difference in TP load between 30 and 60 mm/h was that runoff-yielding time

declined substantially as precipitation intensity increased and the rainfall amount remained the same. The small difference between 90 and 120 mm/h was caused by the limited decrease of runoff-yielding time. The distinct difference between 60 and 90 mm/h probably resulted from the heavier raindrops breaking down the soil particles, which increased the surface area of the soil particles, more adsorbed phosphorus adsorbed to the soil particles, and the soil particles were more easily carried after crushing, thereby increasing the amount of adsorbed phosphorus transport.

The results also indicated that the effects of precipitation intensity on TP load under certain rainfall amount were not obvious when precipitation intensity was between 60 and 90 mm/h. However, precipitation intensity played a major role in TP losses when it was increased from 60 to 90 mm/h.

3.2.2. The Effects of Precipitation Intensity on TP Concentration

The effects of precipitation intensity on TP load was not only affected by precipitation intensity but also affected by rainfall runoff. Therefore, the research method for the effect of precipitation intensity on TP concentration was different from that of TP load. At this time, the precipitation duration was set to constant, and the effects of different precipitation intensities on TP concentration under the same precipitation duration were studied.

The correlation between precipitation intensity and TP concentration in each gradient condition is shown in Figure 7. At this point, the TP concentrations at five gradients were replaced by the mean to eliminate the effect of gradient on TP concentration changes.

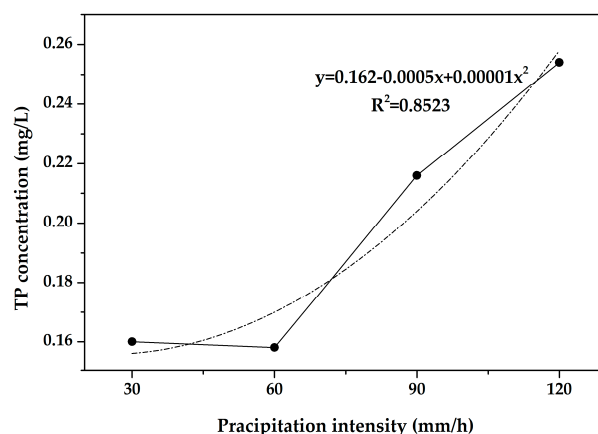


Figure 7. Correlation between precipitation intensity and TP concentration.

According to Figure 7, TP concentration increased with the increase of precipitation intensity, which could be described by quadratic polynomial, and the correlation coefficient was 0.8523. In the process of precipitation, the greater the precipitation intensity, the heavier raindrops per unit time in the soil surface made the soil crushed to increase the surface area of soil particles, which adsorbs more adsorbed phosphorus. Meanwhile, the higher the frequency of soil scour in the area per unit area, the more obvious the role of surface soil by rain erosion, rainfall runoff would cause larger soil erosion, and broken soil particles were more likely to be carried. Therefore, the precipitation duration under certain circumstances, caused by the precipitation intensity change than TP load changes in precipitation should be large, resulting in the increase of TP concentration.

3.3. The Effects of Gradient

3.3.1. The Effects of Gradient on TP Load

Figure 8a shows the TP load generated under different gradients in each precipitation intensity scenario. Figure 8b reflects the effects of gradient on TP load, and the TP loads under different

precipitation intensities were took the average to eliminate the effects of precipitation intensity on the TP load in this figure. The correlation between the gradient and the TP load could be expressed by a quadratic polynomial.

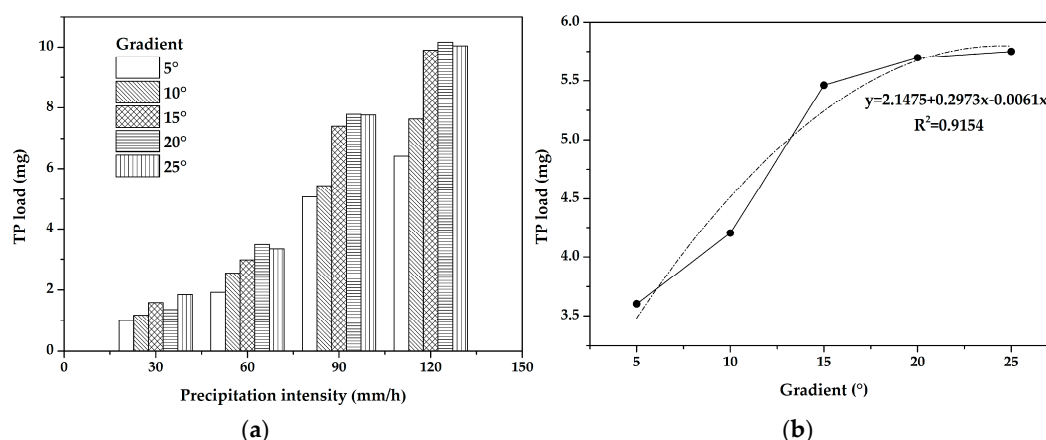


Figure 8. (a) Effect of gradient on TP loads under different precipitation intensities and (b) the correlation between gradient and TP load.

As can be seen from the figure, TP load increased with the increase in gradient, but this increase slowdown after the gradient increased to a certain extent. In the process of precipitation, the scouring effect will be more obvious on the steeper slopes, and precipitation infiltration decreased, rainfall runoff increased, thus carrying more sediments, leading to more serious loss of TP. This phenomenon reflected that there was a critical gradient of the loss of NPS pollutant, indicating that soil erosion and TP loss did not increase with increasing gradient limitlessly. The slight decreases shown in Figure 8a and the declining trend indicated by Figure 8b supports this conclusion that TP load might reach a peak at a certain gradient. Specifically, the TP load decreased slightly as gradient was increased from 20° to 25° under precipitation intensities of 60, 90 and 120 mm/h. This indicates that there was a critical gradient of about 20° for TP loss in the purple soil.

3.3.2. The Effects of Gradient on TP Concentration

Figure 9 shows the correlation between gradient and TP concentration, which can be represented by a quadratic polynomial ($R^2 = 0.7461$). In Figure 9, the four precipitation intensities for each gradient were also averaged to eliminate the influence of precipitation intensity on TP concentration.

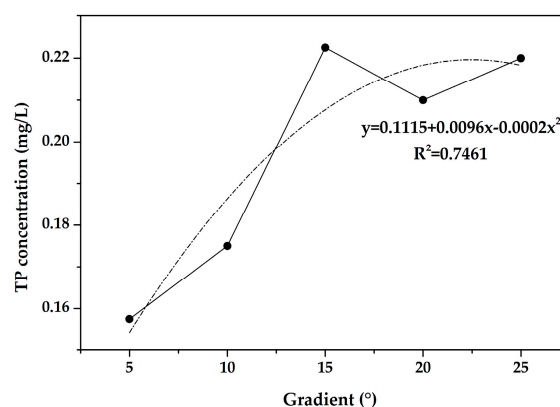


Figure 9. Correlation between gradient and TP concentration.

The positive correlation between gradient and TP concentration was clear when gradient was $<15^\circ$, while the increase in TP concentrations slowed as the gradient was increased, indicating that the TP concentration would not increase limitlessly with increasing gradient. According to the correlation analysis between gradient and TP load, the TP load clearly increased when the gradient was $<15^\circ$. However, the TP loads at gradients of 15° , 20° , and 25° were similar, suggesting that the increases with increasing gradient were small or even negative (Figures 4 and 8).

In addition, for a steeper gradient, the velocity of water flow was faster, the scouring effect stronger, and soil erosion more severe; thus the amount of runoff and sediment that were transported was greater. The increasing runoff and decreasing TP load caused TP concentration to decline when the gradient was $>15^\circ$. This also indicated that there was a critical gradient of TP loss for purple soil, which was similar to the findings of other relevant research. As for the similar concentrations at 15° and 25° , it could be found that TP load was increased with gradient (Figure 8) though the increase was slight when gradient was $>15^\circ$. However, the rainfall runoff at 20° was larger than those of 15° and 25° in some scenarios, which made the TP concentrations could be similar at 15° and 25° . However, the mechanism of how the critical gradient affects TP loss required further research.

4. Conclusions

In this study, we investigated the effects of precipitation and topography conditions on TP loss in purple soil through field experiments. Norton nozzle-type rainfall simulator and specially designed soil boxes were used to simulate precipitation based on 20 scenarios about precipitation (precipitation intensities were 30, 60, 90 and 120 mm/h, and precipitation duration was 40 min) and topography (gradients were 5° , 10° , 15° , 20° , 25°) conditions of natural precipitation.

The results showed that there were positive correlations between rainfall amount and TP load on different gradients. In addition, there was an initial time of runoff and sediment yield before runoff generation, which was different under various precipitation and terrain conditions. Similarly, positive linear relationships could be used to represent the correlations between rainfall amount levels as well as TP concentrations. Moreover, TP load generally increased with increasing precipitation intensity when rainfall amount was limited to a certain duration; however, the difference between TP load at 30 and 60 mm/h was minimal as was that between 90 and 120 mm/h. Similarly, the TP concentration increased with increasing precipitation intensity. In terms of the topographical conditions, the TP load generally increased with gradient but this increase was not limitless. This was indicated by the slight decreases in TP load under a gradient of 25° compared with those under a gradient of 20° under precipitation intensities of 60, 90 and 120 mm/h. Moreover, the positive correlation between gradient and TP concentration was clear at gradients $>15^\circ$; at greater gradients, this increase became more gradual, which indicated there was a critical gradient for TP loss. Combined with changes in the process of TP loss, we determined that 20° was the critical gradient for TP loss from purple soil.

This study reveals the effects of rainfall amount, precipitation intensity, and gradient on TP losses from purple soil, which had not been discussed thoroughly in previous studies, using quantitative correlation analysis. These results provide theoretical support for NPS pollution simulation and pollution control in terms of factors that influence TP loss and their mechanisms. This study was based on an experimental scale, and the probability of extreme precipitation event increased as the climate changing. The minor changes of probabilities were differently manageable according to the range corresponding to the precipitation event, which indicated that a minor climate change maybe cause serious nonpoint pollution [35,36]. In future studies, the concept of the critical gradient for TP loss from purple soil will be further developed, the role of land use in TP loss and the mechanisms underlying TP loss with multiple precipitation events will also be examined.

Acknowledgments: This research work was funded by the National Key Scientific and Technological Projects of the PRC (2014ZX07104-005), and the Fundamental Research Funds for the Central Universities of PRC (JB2014129). The authors gratefully acknowledge the financial support of the programs and agencies.

Author Contributions: Xiaowen Ding conceived and designed the experiments; Ming Lin performed the experiments; Yuan Liu contributed to data measurement; Ying Xue analyzed the data; Xiaowen Ding and Ying Xue wrote the paper.

Conflicts of Interest: The authors declare no conflicts of interest.

References

1. Morales, N.; Boehler, M.A.; Buettner, S.; Liebi, C.; Siegrist, H. Recovery of N and P from Urine by Struvite Precipitation Followed by Combined Stripping with Digester Sludge Liquid at Full Scale. *Water* **2013**, *5*, 1262–1278. [[CrossRef](#)]
2. Orłowski, N.; Lauer, F.; Kraft, P.; Frede, H.-G.; Breuer, L. Linking Spatial Patterns of Groundwater Table Dynamics and Streamflow Generation Processes in a Small Developed Catchment. *Water* **2014**, *6*, 3085–3117. [[CrossRef](#)]
3. Wang, Z.W.; Yang, S.T.; Zhao, C.S.; Bai, J.; Lou, H.Z.; Chen, K.; Wu, L.N.; Dong, G.T.; Zhou, Q.W. Assessment of Non-Point Source Total Phosphorus Pollution from Different Land Use and Soil Types in a Mid-High Latitude Region of China. *Water* **2016**, *8*, 505. [[CrossRef](#)]
4. Piniewski, M.; Marcinkowski, P.; Kardel, I.; Giełczewski, M.; Izydorczyk, K.; Frątczak, W. Spatial Quantification of Non-Point Source Pollution in a Meso-Scale Catchment for an Assessment of Buffer Zones Efficiency. *Water* **2015**, *7*, 1889–1920. [[CrossRef](#)]
5. Alvarez, S.; Asci, S.; Vorotnikova, E. Valuing the Potential Benefits of Water Quality Improvements in Watersheds Affected by Non-Point Source Pollution. *Water* **2016**, *8*, 112. [[CrossRef](#)]
6. Motsinger, J.; Kalita, P.; Bhattarai, R. Analysis of Best Management Practices Implementation on Water Quality Using the Soil and Water Assessment Tool. *Water* **2016**, *8*, 145. [[CrossRef](#)]
7. Yang, S.T.; Dong, G.T.; Zheng, D.H.; Xiao, H.L.; Gao, Y.F.; Lang, Y. Coupling Xinanjiang model and SWAT to simulate agricultural non-point source pollution in Songtao watershed of Hainan, China. *Ecol. Model.* **2011**, *222*, 3701–3717. [[CrossRef](#)]
8. Buchanan, B.; Easton, Z.M.; Schneider, R.L.; Walter, M.T. Modeling the hydrologic effects of roadside ditch networks on receiving waters. *J. Hydrol.* **2013**, *486*, 293–305. [[CrossRef](#)]
9. Wesström, I.; Joel, A.; Messing, I. Controlled drainage and subirrigation—A water management option to reduce non-point source pollution from agricultural land. *Agric. Ecosyst. Environ.* **2014**, *198*, 74–82. [[CrossRef](#)]
10. Mishra, A.; Kar, S. Modeling hydrologic processes and NPS pollution in a small watershed in subhumid subtropics using swat. *J. Hydrol. Eng.* **2012**, *17*, 445–454. [[CrossRef](#)]
11. Zheng, Y.; Luo, X.L.; Zhang, W.; Wu, X.; Zhang, J.; Han, F. Transport mechanisms of soil-bound mercury in the erosion process during rainfall-runoff events. *Environ. Pollut.* **2016**, *215*, 10–17. [[CrossRef](#)] [[PubMed](#)]
12. Pan, B.Z.; Wang, H.Z.; Ban, X.; Yin, X.A. An exploratory analysis of ecological water requirements of macroinvertebrates in the Wuhan branch of the Yangtze River. *Quat. Int.* **2015**, *380*, 256–261. [[CrossRef](#)]
13. Kang, L.; Zhang, H.Q. A comprehensive study of agricultural drought resistance and background drought levels in five main grain-producing regions of China. *Sustainability* **2016**, *8*, 346. [[CrossRef](#)]
14. Zhong, X.H.; Cheng, G.W.; Li, Y. A study of forest hydrologic effect in the Sichuan basin region of the upper reaches of the Yangtze River. *Arch. Agron. Soil Sci.* **2010**, *48*, 319–327.
15. Lou, H.Z.; Yang, S.T.; Zhao, C.S.; Zhou, Q.W.; Bai, J.; Hao, F.H.; Wu, L.N. Phosphorus risk in an intensive agricultural area in a mid-high latitude region of china. *Catena* **2015**, *127*, 46–55. [[CrossRef](#)]
16. Zhou, Y.; Luo, M. Texture Statistics for Sichuan Basin Terrain Morphology Analysis DEM Based. In Proceedings of the International Conference on Machine Vision and Human-Machine Interface, Luoyang, China, 24–25 April 2010; pp. 319–322.
17. Niu, J.; Zhang, P.C.; Xing, M.X. Characteristics of soil and water loss on purple slope farmland and its control in upper reaches of the Yangtze River. *Sci. Soil Water Conserv.* **2010**, *8*, 64–68. (In Chinese).
18. Wang, B.; Zheng, F.; Römkens, M.J.M.; Darboux, F. Soil erodibility for water erosion: A perspective and Chinese experiences. *Geomorphology* **2013**, *187*, 1–10. [[CrossRef](#)]
19. Zhang, J.H.; Wang, Y.; Li, F.C. Soil organic carbon and nitrogen losses due to soil erosion and cropping in a sloping terrace landscape. *Soil Res.* **2015**, *53*, 87–96. [[CrossRef](#)]

20. Gao, Y.; Zhu, B.; Yu, G.R.; Chen, W.L.; He, N.P.; Wang, T.; Miao, C.Y. Coupled effects of biogeochemical and hydrological processes on C, N, and P export during extreme rainfall events in a purple soil watershed in southwestern China. *J. Hydrol.* **2014**, *511*, 692–702. [[CrossRef](#)]
21. Sharma, R.; Bell, R.W.; Wong, M.T.F. Phosphorus forms in soil solution and leachate of contrasting soil profiles and their implications for P mobility. *J. Soils Sediments* **2015**, *15*, 854–862. [[CrossRef](#)]
22. Kollongei, K.J.; Lorentz, S.A. Modelling hydrological processes, crop yields and NPS pollution in a small sub-tropical catchment in South Africa using ACRU-NPS. *Hydrol. Sci. J.* **2015**, *60*, 2003–2028. [[CrossRef](#)]
23. Nie, X.J.; Zhang, J.H.; Gao, H. Soil enzyme activities on eroded slopes in the Sichuan Basin, China. *Pedosphere* **2015**, *25*, 489–500. [[CrossRef](#)]
24. Ding, X.W.; Shen, Z.Y.; Liu, R.M.; Chen, L.; Lin, M. Effects of ecological factors and human activities on nonpoint source pollution in the upper reach of the Yangtze River and its management strategies. *Hydrol. Earth Syst. Sci. Discuss.* **2013**, *11*, 691–721. [[CrossRef](#)]
25. Shin, M.H.; Won, C.H.; Jang, J.R.; Choi, Y.H.; Shin, Y.C.; Lim, K.J.; Choi, J.D. Effect of surface cover on the reduction of runoff and agricultural NPS pollution from upland fields. *Paddy Water Environ.* **2013**, *11*, 493–501. [[CrossRef](#)]
26. Boluwade, A.; Madramootoo, C. Determining the influence of land use change and soil heterogeneities on discharge, sediment and phosphorus. *J. Environ. Inform.* **2014**, *25*, 126–135. [[CrossRef](#)]
27. Wang, J.; Pant, H. Land use impact on bioavailable phosphorus in the Bronx River, New York. *J. Environ. Prot.* **2011**, *2*, 342–358. [[CrossRef](#)]
28. Sharpley, A.N.; Kleinman, P.J.; Heathwaite, A.L.; Gburek, W.J.; Folmar, G.J.; Schmidt, J.P. Phosphorus loss from an agricultural watershed as a function of storm size. *J. Environ. Qual.* **2008**, *37*, 362–368. [[CrossRef](#)] [[PubMed](#)]
29. Qian, J.; Zhang, L.P.; Wang, W.Y.; Liu, Q. Effects of vegetation cover and slope length on nitrogen and phosphorus loss from a sloping land under simulated rainfall. *Pol. J. Environ. Stud.* **2014**, *23*, 835–843.
30. Gao, Y.; Zhu, B.; Zhou, P.; Tang, J.L.; Wang, T.; Miao, C.Y. Effects of vegetation cover on phosphorus loss from a hillslope cropland of purple soil under simulated rainfall: A case study in China. *Nutr. Cycl. Agroecosyst.* **2009**, *85*, 263–273. [[CrossRef](#)]
31. Volf, C.A.; Ontkean, G.R.; Bennett, D.R.; Chanasyk, D.S.; Miller, J.J. Phosphorus losses in simulated rainfall runoff from manured soils of Alberta. *J. Environ. Qual.* **2007**, *36*, 730–741. [[CrossRef](#)] [[PubMed](#)]
32. Huang, J.; Wu, P.; Zhao, X.N. Effects of rainfall intensity, underlying surface and slope gradient on Soil infiltration under simulated rainfall experiments. *Catena* **2013**, *104*, 93–102. [[CrossRef](#)]
33. Hengren, L.F.; Goonetilleke, A.; Sukpum, R.; Silva, D.Y.D. Rainfall Simulation as a Tool for Urban Water Quality Research. *Environ. Eng. Sci.* **2005**, *22*, 378–383. [[CrossRef](#)]
34. Zhang, J.H.; Su, Z.A.; Liu, G.C. Effects of terracing and agroforestry on soil and water loss in hilly areas of the Sichuan Basin, China. *J. Mt. Sci.* **2008**, *5*, 241–248. [[CrossRef](#)]
35. Djebou, S.; Dagbegnon, C.; Singh, V.P. Impact of climate change on precipitation patterns: A comparative approach. *Int. J. Climatol.* **2016**, *36*, 10.
36. Djebou, D.C.S.; Singh, V.P.; Frauenfeld, O.W. Analysis of watershed topography effects on summer precipitation variability in the southwestern United States. *J. Hydrol.* **2014**, *511*, 838–849. [[CrossRef](#)]

